

### Chemical properties of *n*-ZnO/*p*-CuO heterojunctions for photovoltaic applications

B. B. Dhale<sup>a</sup>, S. H. Mujawar<sup>b</sup>, S. L. Bhattar<sup>a\*</sup> and P. S. Patil<sup>c</sup>

<sup>a</sup>Gogate Jogalekar College, Ratnagiri, (M.S), India

<sup>b</sup>Mahatma Phule Mahavidhyalaya, Pimpri, Pune (M.S), India

<sup>c</sup>Thin Film Materials Laboratory, Department of Physics, Shivaji University, Kolhapur, (M.S.) India

#### ABSTRACT

Polycrystalline heterojunctions of *n*-ZnO and *p*-CuO were fabricated. The *n*-ZnO (*d*~800 nm) was prepared at optimized substrate temperature of 450°C onto the F:SnO<sub>2</sub> coated glass substrate by spray pyrolysis technique. The *n*-ZnO layer was followed by a layer of *p*-CuO (*d*~400 nm), which was prepared by vacuum evaporation technique. The structural and morphological properties of individual layers were studied. Band energy diagrams corresponding to these junctions would be needed to understand their properties and these are not available. In the paper, synthesized band energy diagrams of these heterojunctions are purposed based on reported experimental data. The heterojunction (Ag/*p*-CuO/*n*-ZnO/F:SnO<sub>2</sub>) so formed as subjected to annealing at different temperatures such as 100, 200, 300, 400 and 500°C. I-V characteristics of these junctions in dark and under visible light illumination were studied systematically. The heterojunction annealed at 200°C was found to give better electrical response as compared to other studied heterojunction.

**Key words:** Heterojunctions, Ag/*p*-Cu<sub>2</sub>O/*n*-ZnO/F:SnO<sub>2</sub>, I-V characteristics

#### INTRODUCTION

p-n junctions are the key technology in many electronic and optoelectronic devices. Oxide semiconductors either exhibit n- or p-type conductivity. Zinc oxide is an n-type semiconductor with an energy gap of about 3.3 eV and conductivities of about 10<sup>-7</sup>-10<sup>-3</sup> Scm<sup>-1</sup> [1, 2]. On the other hand, cupric oxide (CuO) a direct-gap semiconductor with a 1.7 eV band-gap is an unipolar p-type material and has not been well investigated in detail to date regarding growth methods, as well as for control of electrical and optical properties. CuO is an attractive material for photovoltaic applications since it has advantages of a relatively high absorption coefficient in the visible region, low-cost production, and is non-toxic, and is fabricated from abundantly available materials. It should be possible to make better solar cells using a heterojunction between CuO and a n-type TCO (Transparent Conducting Oxide). Recently the ZnO/CuO heterojunction have shown a considerable improvement [3, 4]. Among all possible combinations. Fabricated a *p*-CuO/*n*-ZnO thin film heterojunction on a glass substrate by the sol-gel technique [5]. Polycrystalline *n*-ZnO/*p*-Cu<sub>2</sub>O heterojunctions by reactive sputtering for photovoltaic applications. [6]. As a result of the new research efforts, cells with photovoltaic conversion efficiencies as high as 2%.J. [7] studied the fabrication and the characterization of heterojunction solar cells based on electrodeposited ZnO and Cu<sub>2</sub>O. The effect of the electrodeposition conditions (pH and temperature) on the cell performance has been investigated. The cell made with

a Cu<sub>2</sub>O layer deposited at high pH and moderate temperature (50°C), have shown the conversion efficiency as high as 0.41%.

In this paper, we report on a *n*-ZnO and *p*-CuO thin film heterojunction fabricated. The *n*-ZnO was prepared at optimized substrate temperature of 450°C onto the F:SnO<sub>2</sub> coated glass substrate by spray pyrolysis technique. The *n*-ZnO layer was followed by a layer of *p*-CuO, which was prepared by vacuum evaporation technique. The I-V characteristics show thermally activated diode-like rectifying behaviour and also we synthesized band energy diagrams of these heterojunction are purposed based on calculated experimental data.

## MATERIALS AND METHODS

The *p*-CuO/*n*-ZnO heterojunctions were fabricated using two different techniques: spray pyrolysis technique (SPT) and vacuum deposition technique (VDT). Initially, the solution for deposition of zinc oxide (ZnO) thin film was prepared by dissolving 10.975 gm of zinc acetate [Zn(CH<sub>3</sub>CO)<sub>2</sub>·2H<sub>2</sub>O] in 100 ml double distilled water. The concentration of this zinc acetate solution is 0.5 M. The films were deposited on to the conducting fluorine doped tin oxide (FTO) coated glass substrates. Prior to deposition, the substrates were cleaned ultrasonically, first in chromic acid and subsequently in methanol for 10-15 min each and then treated with acetone. The thin films of ZnO were prepared by SPT at a deposition temperature of 400°C. The thicknesses of the films were measured by AMBIOS make XP-1 surface profiler and were found to be in the range of 0.332-0.457 μm. The physical structure of the films viz. crystalline structure and phase identification were investigated by X-ray diffraction (XRD) studies of thin films using CuKα (λ=1.54056 Å) radiations. The surface morphology of films was studied by using JEOL-JSM 6360 scanning electron microscope (SEM). The optical absorption studies of the deposited films were investigated using dual beam UV-Vis spectrometer (Systronics 119) in the wavelength range of 350-850 nm. In addition to this, the conductivity of ZnO film was decided by thermoelectric power (TEP) measurements. The ZnO film thus prepared on FTO coated glass was used as a substrate for the deposition of copper oxide layer in order to achieve the heterojunction. The deposition of copper (Cu) metal on ZnO was carried out using VDT followed by annealing at different temperatures to achieve *p*-type cupric oxide (CuO).

After synthesizing the *p*-CuO/*n*-ZnO heterostructure, it was further characterized by XRD and SEM in order to decide the formation of desired material in *p*-*n* heterostructure. The *p*-*n* junction thus formed, was subjected to I-V characterization to decide the true synthesis of *p*-*n* heterojunction

## RESULTS AND DISCUSSION

### 1.1. X-ray diffraction (XRD)

The structural and phase identification for the desired material were studied with the help of XRD technique. The angle of diffraction (2θ) is varied between 10-100°. Figure 2 shows the XRD pattern for the *p*-CuO/*n*-ZnO heterojunction annealed at 400°C. The observed XRD patterns are compared with standard JCPDS data file (File Nos. 05-0664 ZnO, 80-1917 CuO, 01-1142 Cu<sub>2</sub>O, 82-2194 Sn<sub>4</sub>O<sub>6</sub>), matching the observed *d*-values with that of standard ones.

The XRD pattern shows prominent reflections along (100), (002) planes respectively at 2θ=32.5, 34.4° for ZnO and (111) plane at 2θ=38.3° for CuO. Apart from these peaks, other peaks such as (002), (100), (101), (103) for ZnO and (111), (021), (113) for CuO are seen. The presence of these planes ensures the true deposition of the desired materials *n*-ZnO and *p*-CuO respectively, without forming any other detrimental phases. Thus XRD analysis confirmed the phases of *n*-ZnO and *p*-CuO [8]. They show the peaks that can be assigned to either to hexagonal wurtzite ZnO or monoclinic tenorite phase.

### 1.2. Surface morphology

Figure 3(a-c) shows the surface morphology of the *p*-CuO and *n*-ZnO junction and the cross-sectioned structure of the heterojunction examined using scanning electron microscope. The ZnO layer was flat in morphology. The CuO layers were composed of grains grown and the grain size was 200-300 nm. SEM images of CuO, ZnO and CuO/ZnO heterojunction annealed at 400°C at a magnification of X220. The heterointerface between the ZnO and the CuO layers could be clearly observed.

### 1.3. Construction of energy band diagram

Schematics of the band diagram of a p-n junction for *n*-ZnO and *p*-CuO is shown in Figure 4. The energy difference between the Fermi level and the valence band (*p*-type),  $\delta_p$ , or the conduction band edge (*n*-type),  $\delta_n$ , for each oxide is obtained from their carrier densities as [9]

$$p = 2 \left( \frac{2\pi m^* kT}{h^2} \right) e^{\left( \frac{\delta_p}{kT} \right)} \quad \dots\dots\dots (1)$$

$$n = 2 \left( \frac{2\pi m^* kT}{h^2} \right)^{3/2} e^{\left( \frac{\delta_n}{kT} \right)} \quad \dots\dots\dots (2)$$

where  $m^*$  is the effective mass,  $k$  is the Boltzmann constant,  $T$  is the temperature and  $h$  is the Planck's constant. Table 1 shows the data of carrier concentrations, electron affinity ( $\chi$ ), band gap energy ( $E_g$ ), and the work function, ( $\phi$ ). The  $\delta_p$  and  $\delta_n$  values deduced from equations 6.4 and 6.5 are listed in Table 1.

The electronic behavior of a heterojunction is similar to that of a homojunction except for new boundary conditions which cause jumps of band edges at the interface. These jumps originate from the band offsets, effective mass, carrier mobility and the dielectric constant discontinuities. A rectifying barrier is formed at these p-n heterojunctions due to the existence of charge depletion region, as found experimentally for CuO-ZnO [10].

Diffusion potentials were obtained, using their respective work function data, as below and are listed in Table 2:

$$V_D = (\phi_p - \phi_n) \quad \dots\dots\dots (3)$$

Using this  $V_D$  value, the conduction band edge discontinuity  $\Delta E_c$  for each junction is determined from the relation:

$$\Delta E_c = E_{gp} - V_D - \delta_p - \delta_n \quad \dots\dots\dots (4)$$

where  $E_{gp}$  is the energy gap of the *p*-type semiconductor. The  $\Delta E_c$  values thus calculated are presented in Table 2.

### 1.4. Current-Voltage (I-V) characteristics

Figure.5 shows the typical I-V characteristics of the *p*-CuO/*n*-ZnO heterojunction (annealed at 400°C temperatures) recorded under dark and under light illumination (center wavelength 365 nm) 0.31 W/cm<sup>2</sup> intensity in a two electrode configuration. An increase in the current is observed when films are illuminated under applied voltage. The photo response upon illumination indicates that the films are sensitive to light, (photoactive) thereby supporting the semiconductor behavior. For samples annealed at 200 and 300°C, there is relatively small conduction of current through the circuit. A rectifying characteristic similar to a conventional p-n junction is observed with very reproducible characteristics for ZnO-Cu<sub>2</sub>O and ZnO-CuO heterojunction. The forward current is increased exponentially while the reverse current shows a very little increment; the diode-like I-V characteristics confirm the formation of the *p-n* photo active heterojunction at the interface of ZnO and CuO. This result is consistent with the *p*-type and *n*-type conductivities of CuO and ZnO respectively.

Power incident on heterojunction is = 0.31 W/cm<sup>2</sup>

Hence, it is clear from the I-V characteristics that the heterojunction made up of *p*-CuO/*n*-ZnO (annealed at 400°C)

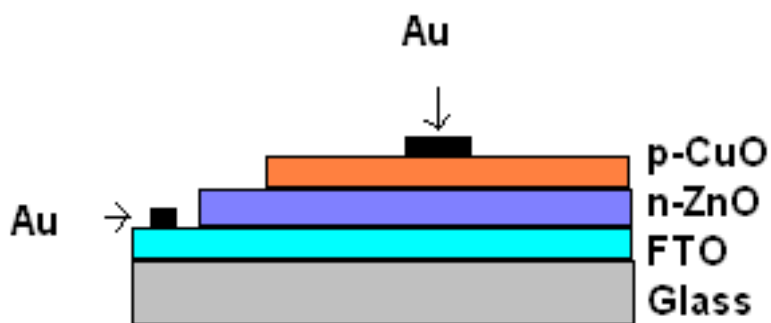


Figure 1 Schematic of a *p*-CuO/*n*-ZnO heterojunction device. 'Au' is used for ohmic contacts

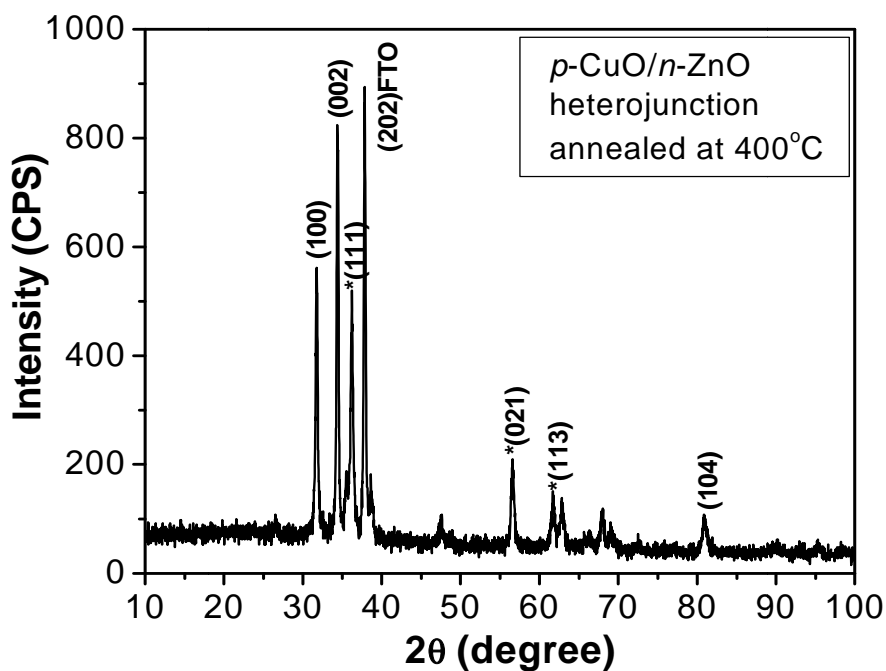
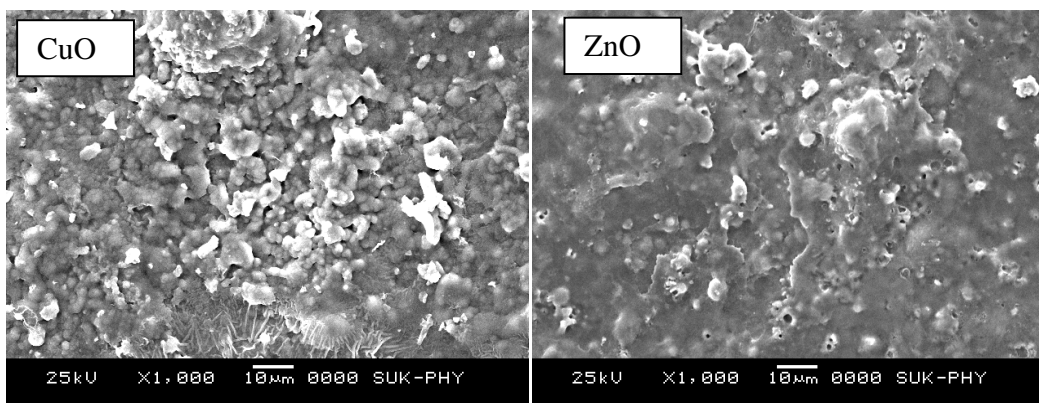


Figure 2 XRD pattern for the *p*-CuO/*n*-ZnO heterojunction annealed at a temperature of 400°C. The planes preceding '\*' denote the peaks of CuO



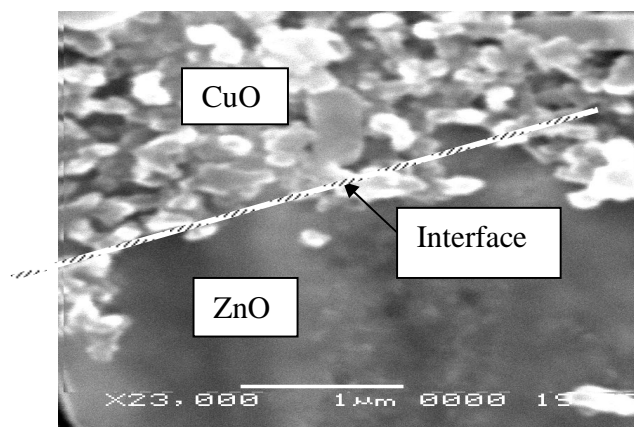
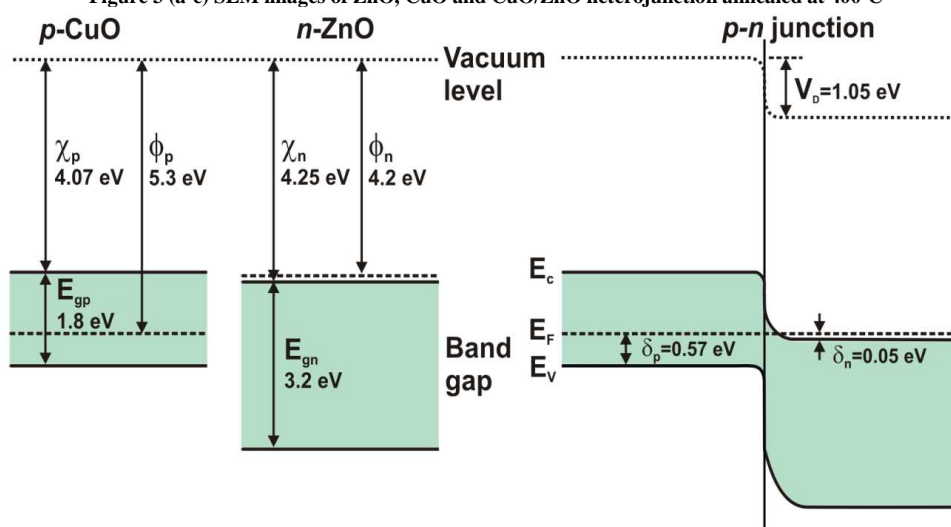


Figure 3 (a-c) SEM images of ZnO, CuO and CuO/ZnO heterojunction annealed at 400°C



$E_F$  – Fermi level,  $E_v$  – Upper level of valence band,  $E_c$  – Lower level of conduction band,  $V_D$  – Diffusion potential,  $\phi$  – Work function,  $\delta$  – Energy difference between Fermi level and conduction / valence band edge,  $\chi$  – Electron affinity

Figure 4 Band diagrams of the isolated states of *p*-CuO, *n*-ZnO and the *p*-CuO/*n*-ZnO heterojunction under equilibrium condition

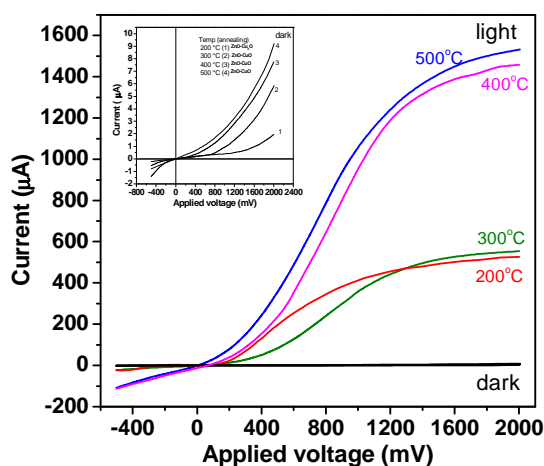


Figure 5 I–V characteristics of (1) ZnO-Cu<sub>2</sub>O, (2) ZnO-CuO, (3) ZnO-CuO and (4) ZnO-CuO annealed at 200, 300, 400 and 500°C respectively, under dark and light illumination. Power of illuminating mercury lamp: 250 W/cm<sup>2</sup>. Inset shows I–V response dark for all the heterojunctions

Table 1 Various parameters of heterojunction *p*-CuO/*n*-ZnO

Semiconducting Oxide	Carrier conc. (cm <sup>-3</sup> )	Electron affinity, $\chi$ (eV)	Energy gap, $E_g$ (eV)	Work Function, $\phi$ (eV)	$\delta_n$ (eV)	$\delta_p$ (eV)
<i>p</i> -CuO	$2.1 \times 10^{17}$	4.07	1.8	5.3	-----	0.12
<i>n</i> -ZnO	$3.2 \times 10^{21}$	4.2	3.2	4.25	0.05	-----

Table 2 Calculated values of  $\Delta E_c$  and  $V_D$  for heterojunction *p*-CuO/*n*-ZnO

Heterojunction	$\Delta E_c$ (eV)	$V_D$ (eV)
CuO	0.625	1.05

### CONCLUSION

*n*-ZnO and *p*-CuO heterojunctions were fabricated for photovoltaic applications. XRD analysis confirmed the phases of *n*-ZnO and *p*-CuO. The micrograph shows the fine edge between two layers of heterostructure. The SEM study has revealed that films under investigation are highly dense and compact in nature that means these samples in general exhibit lower degree of porosity. The I-V characteristics of heterojunction under dark and illumination condition have been measured using potentiostat -II perkin-Elmer with three electrode electrochemical cell. Incident light of 0.31 W/cm<sup>2</sup> power generates photocurrent of magnitude 1.6mA. When coupled through 1k $\Omega$  load resistance, it generates about 1.6V across it. This photovoltage is applied to the working electrode of EC cell. Further work in this direction is ongoing in our group.

### Acknowledgments

The authors would like to thank for common facility centre and Department of Physics in Shivaji University, Kolhapur, for the X-ray diffraction and SEM, Current-Voltage (I-V) measurement respectively.

### REFERENCES

- [1] Parreta A., Jayaraj M. K., Di Nocera A., Loreti S., Quercia L., and Agati A., *phys. stat. sol. (a)* **1996**,155, 399
- [2] Olsen L. C., Addis F. W., and Miller W., *Sol. Cells*,**1982–1983**. 7, 247
- [3] Minami T., Miyata T., Ihara K., Minamino Y., Tsukada S., *Thin Solid Films*, **2006**, 494, 47
- [4] Mittiga A., Salza E., Sarto F., Tucci M., Vasanthi R., *Appl. Phys. Lett.*, **2006**, 88, 163502.
- [5] Mridha S. and Basak D., *Semicond. Sci. Technol.* 21 (**2006**) 928.
- [6] Ishizuka S., Suzuki K., Okamoto Y., Yanagita M., Sakurai T., Akimoto K., Fujiwara N., Kobayashi H., Matsubara K. and Niki S., *Phys. Stat. Sol. (c)* 1 (**2004**) 1067.
- [7] Jeong S.S., Mittiga A., Salza E., Masci A. and Passerini S., *Electrochim. Acta* 53 (**2008**) 2226.
- [8] Van Ruyven, *J. Appl. Phys.* 50. 8/98 (**1979**) 1063.
- [9] Alexander M., Bukowski T.P., Uhlmann, D. Teowee R., McCarthy G., Dawley K.C., Zelinski J., Hutson B.J.J A.R., *Phys T.J. Rev.* 108 (**1957**) 222.
- [10] Nakamura S., Mridha S. and Basak D., *J. Electrochem. Soc.* 137 (**1990**) 940.